applied sciences

MDPI

Article

Comparative Environmental Evaluation of Conventional, Low-Clinker and Alkali-Activated Concretes and Mortars

Beata Łaźniewska-Piekarczyk *, Patrycja Miera, Mateusz Moskal and Robert Domin

Department of Building Engineering and Building Physics, Faculty of Civil Engineering, Silesian University of Technology, Akademicka 5, 44-100 Gliwice, Poland; patrycja.miera@polsl.pl (P.M.)
* Correspondence: beata.lazniewska-piekarczyk@polsl.pl

Abstract

Clinker substitution can reduce cradle-to-gate global warming potential (GWP), but does not establish improvement in resource depletion, toxicity, or ecotoxicity. This life cycle assessment (LCA) compares six concrete and four mortar inventory models per 1 m^3 at the production gate using the Swiss Federal Office for the Environment (BAFU) inventory and the CML baseline life cycle impact assessment method (CML-IA), developed by Leiden University's Institute of Environmental Sciences (CML). Under the original provider mappings, AAC-3 (slag–fly ash alkali-activated concrete) had the lowest modeled GWP within the concrete group at 78.2 kg CO_2 eq m^{-3}, 71.9% below concrete CEM I (278.2 kg CO_2 eq m^{-3}). CEM III/C mortar had the lowest modeled GWP within the mortar group at 101.2 kg CO_2 eq m^{-3}, 76.6% below mortar CEM I (433.1 kg CO_2 eq m^{-3}). These are separate 1 m^3 production gate results using the original activator exchanges, a common freight exchange, and no additional curing energy; they do not establish performance equivalence. CEM II/B-V concrete was below its reference in all eleven categories, whereas activated models exceeded their references in seven or eight. Clinker dominated GWP in the CEM I reference systems; natural gas was the largest positive GWP process in the activated models (7.8–12.4% of net GWP). The modeled mercury cell, sodium hydroxide and upstream mercury supply processes accounted jointly for 32.3–72.4% of activated system terrestrial ecotoxicity. Activator mappings and precursor allocation remain unresolved, so these results identify the lowest outputs in the original models rather than a validated ranking of materials.

Keywords: life cycle assessment; process contribution analysis; clinker reduction; alkali-activated materials; environmental burden shifting; Pareto dominance; hotspot concentration; CML-IA baseline

Check for updates

Academic Editor: Paulo Santos

Received: 23 September 2026
Revised: 20 October 2026
Accepted: 2 November 2026
Published: 4 November 2026

Copyright: © 2026 by the authors. Licensee MDPI, Basel, Switzerland. This article is an open access article distributed under the terms and conditions of the Creative Commons Attribution (CC BY) license.

1. Introduction

Cementitious materials are produced at a scale that makes their environmental performance consequential for construction sector decarbonization. A substantial part of the global warming potential (GWP) of Portland cement products originates before the concrete or mortar reaches the construction site. Carbon dioxide is released directly during carbonate calcination and indirectly through the energy required to manufacture clinker [1–5]. Reducing the mass of clinker per unit of product is consequently one of the main technological routes for lowering production stage greenhouse gas emissions. This route includes the use of Portland cements with supplementary main constituents, such as fly ash, ground granulated blast furnace slag (GGBFS), and limestone [3,5–7].

Clinker reduction does not define a single material or environmental profile. CEM II, CEM III, and multicomponent cements can differ in clinker fraction, supplementary constituents, processing requirements, and performance [3,6,7]. Alkali-activated materials extend the design space further by replacing most or all Portland clinker with aluminosilicate precursors activated by alkaline solutions [8,9]. GGBFS, fly ash, and their blends are among the most widely studied precursors, whereas sodium hydroxide, sodium silicate, potassium hydroxide, or combinations of these chemicals may be used as activators [8–10]. Avoiding clinker can reduce GWP, but the associated inventory can shift towards precursor processing, activator manufacture, electricity, thermal energy, transport, and background chemical supply chains [10–14].

Life cycle assessment (LCA) provides a consistent framework for quantifying such shifts. Comparative studies commonly report GWP because it is policy-relevant and readily interpretable, but the result does not represent overall environmental performance. Midpoint indicators for resource depletion, acidification, eutrophication, toxicity, ecotoxicity, ozone depletion, and photochemical oxidation describe different environmental mechanisms and use different reference units. Lower GWP may therefore coincide with higher results in one or more other categories [10,12–14]. Reviews of alkali-activated material LCAs have also identified strong methodological heterogeneity in functional units, system boundaries, geographical representation, inventory databases, allocation rules, activator datasets, and transport assumptions [12]. Reported percentages cannot be transferred from one model to another without accounting for these choices.

Prior mixture-level LCAs report multi-category results; some also identify major contributors [15,16]. The gap addressed here is linking cross-category screening to the sign and concentration of underlying process contributions. Without this link, burden shifting shows where category results differ but not whether a hotspot is concentrated in one process, offset by negative corrections, or distributed across linked supply chains. A concentrated result directs checks to particular exchanges; a diffuse result calls for tracing connected providers. This workflow makes apparent advantages traceable to inventory assumptions requiring verification before material selection, while keeping positive contributions distinct from the net category score.

The wider concrete LCA literature shows that apparently similar low-carbon mixtures can yield different conclusions when inventory completeness, geography, functional equivalence, or the treatment of supplementary cementitious materials changes [17–22]. Studies of waste-containing and pozzolanic concretes similarly show that the environmental advantage of substitution depends on the selected material, replacement level, supply chain, and set of impact indicators [23,24]. These findings make the model structure and the basis of comparison as important as the reported GWP percentage.

Multifunctionality is a particularly consequential source of variation. Blast furnace slag and other industrial co-products may be represented using cut-off, allocation, substitution, or market-responsive approaches, and these choices can materially change the burden assigned to the binder system [21,25,26]. System boundary completeness can also matter: hybrid and process-based assessments of cement, concrete, and geopolymer concrete do not necessarily produce the same carbon intensities [27]. A further source of non-comparability is the use of a purely volumetric functional unit where the mixtures differ in strength, exposure class, durability, or service life [18,21].

Recent mixture-level studies have expanded the evidence for activated concretes and mortars under different inventories, transport conditions, exposure contexts, and side stream compositions [28–31]. Their results repeatedly identify activator technology and dosage as influential, while waste-derived activators can reduce impacts associated with commercial sodium silicate or hydroxide production [29,32–34]. Published inventories for sodium

silicate and earlier carbon assessments of alkali-activated concrete further demonstrate that the chemical supply chain is not a negligible or universal constant [35,36]. The present study therefore treats provider-specific process contributions as model results requiring explicit interpretation rather than as inherent properties of an entire binder class.

A further issue is environmental burden shifting. A GWP reduction does not establish improvement across other indicators, and category counts do not express the magnitude or importance of the individual changes. Pareto screening identifies a relation in which one model has no higher impact in any selected category and a strictly lower impact in at least one. This avoids category weighting, but the result is conditional on the inventory and indicator set. It cannot establish technical substitutability, statistical significance or robustness to changes in model assumptions.

The present study examines ten predefined inventory models: six concretes based on CEM I, CEM II/B-V, CEM III/B, alkali-activated ground granulated blast furnace slag, alkali-activated fly ash, or an activated slag–fly ash blend; and four mortars based on CEM I, CEM III/C, CEM VI (S-LL), or alkali-activated slag. Concrete and mortar are screened separately against their own CEM I reference, on a declared unit basis of 1 m^3. The binder designations identify modeled formulations, not verified commercial cement products.

This study addresses three research questions:

1. How do the ten variants compare in GWP and in the direction of change across eleven CML-IA baseline categories?
2. Which variants are Pareto-dominated within the concrete and mortar groups?
3. How concentrated or diffuse are the process-level contributions, and which named processes form the principal hotspots in GWP and selected resource-, toxicity-, and ecotoxicity-related categories?

The methodological contribution is an inventory audit workflow that first checks the mass balance implied by activator solution concentrations and then links four analytical steps: eleven-category comparison, conditional within-group Pareto screening, signed process reconciliation, and hotspot concentration measures D_1, C_5, and N_{80}. The mass balance check separates dry hydroxide and silicate solids from solution water but cannot establish the oxide composition of commercial sodium silicate. Retaining negative entries distinguishes net category results from positive-only concentration measures. Together, these checks trace apparent category trade-offs to inventory assumptions that require verification before material selection. The workflow adds no LCIA factors or category weighting; unresolved provider and recipe mappings still preclude validated comparison of the corresponding physical mixtures.

2. Materials and Methods

2.1. Goal, Scope, and Comparative Design

The assessment followed the goal and scope, inventory, impact assessment, and interpretation structure of ISO 14040 and ISO 14044 [37,38]. Its goal was to compare the production-stage environmental profiles of conventional, low-clinker, and alkali-activated cementitious composites and to determine how the process structure underlying those profiles differed between binder systems. The intended application is comparative environmental screening and hotspot identification at the material production stage. The results are not a whole life assessment and are not intended to certify technical equivalence among the mixtures.

Two product groups were modeled independently. The concrete group contained six variants: CEM I, CEM II/B-V, CEM III/B, AAC-1 GGBFS, AAC-2 fly ash, and AAC-3 GGBFS + fly ash. The mortar group contained four variants: CEM I, CEM III/C, CEM VI

(S-LL), and AAS GGBFS. Each foreground process delivered 1 m^3 of the relevant material as its quantitative reference. Comparisons with CEM I, percentage reductions, category directions, and dominance relations were calculated separately for concrete and mortar. Absolute results from the two groups are reported but are not interpreted as a functional comparison between concrete and mortar.

The model was deterministic. No probability distributions, Monte Carlo calculation, alternative allocation scenario, provider scenario, or transport scenario were introduced. No normalization, weighting, endpoint conversion, or aggregation of impact categories was performed.

2.2. Declared Unit and System Boundary

The declared unit was 1 m^3 of concrete or 1 m^3 of mortar at the production gate. Cement, clinker, precursors and activators were mass inputs to these product systems, reported in kg per m^3; no cement-only result per ton is presented. If a provider is expressed per ton, its activity is the required mass in kg divided by 1000. The boundary included constituent production, linked background supply chains, mixing and the common production-related exchanges. Delivery beyond the modeled freight exchange, placement, site curing, use, maintenance, carbonation, demolition, recycling and disposal were excluded. No common strength, workability, durability or service life requirement was established; the declared unit therefore does not demonstrate functional equivalence.

Each original foreground model contained 42.21 t·km of road freight per declared unit. This is a common modeling input, not a constituent-specific transport inventory. Equal freight exchanges neither represent equal real supply chains nor establish robustness of the ranking. A route-based recalculation would use $T = \Sigma(m_j d_j/1000)$, where m_j is the transported mass in kg per m^3 and d_j is the distance in km; each transport mode requires its own provider. This sensitivity has not been calculated, so the results cannot support conclusions about actual Polish delivery distances.

2.3. Material Systems and Foreground Inventories

Table 1 records the original model inputs. Concrete CEM I, AAC-1 and AAC-3 were adapted from formulations in Garces et al. [14]; the CEM II/B-V and CEM III/B concrete inputs were based on Tait and Cheung [15]. Published impact results were not imported. The NaOH pellet masses taken from [14] were linked, without concentration conversion, to a 50% aqueous provider. Consequently, AAC-1 and AAC-3 represent neither chemically equivalent reproductions of those recipes nor corrected activator inventories. Their reported impacts are retained as outputs of the original model and require recalculation before quantitative material comparisons. AAC-2 was based on the study-specific recipe used in the original model.

All original models included 4.17×10^{-7} item of mixing plant infrastructure, 0.4 MJ of diesel use in construction machinery, 4.3 kWh of medium-voltage electricity, 8.2 MJ of light fuel oil, 0.02 kg of lubricating oil, 5.7 MJ of natural gas and 42.21 t·km of road freight. No additional thermal curing energy was entered. This omission is a boundary assumption and does not establish that all activated mixtures achieve their required performance under ambient curing. No common verified curing regime or 28-day strength dataset is available in this analysis.

Aggregate and separately added water quantities varied among mixtures. For the concretes, sand ranged from 588 to 800 kg m^{-3}, gravel from 1013 to 1170 kg m^{-3}, and separately added water from 96 to 220 kg m^{-3}. The mortars contained 1410 or 1540 kg m^{-3} of sand and 235 or 257 kg m^{-3} of separately added water. Exact per-mixture aggregate

and water quantities are not reproduced in this manuscript. Water contained in activator solutions was additional to the separately entered water exchange.

Table 1. Analyzed product systems and principal binder-related foreground inputs per 1 m^3.

Group	Variant	Principal Binder/Precursor Inputs (kg/m^3)	*Original Activator Exchanges (kg/m^3)*
Concrete	CEM I	CEM I: 354	—
	CEM II/B-V	CEM I: 247; fly ash: 133	—
	CEM III/B	CEM I: 114; GGBFS: 266	—
	AAC-1 GGBFS	GGBFS: 354	NaOH (50%): 4; sodium silicate (48%): 72
	AAC-2 fly ash	Fly ash: 414	NaOH (50%): 104; sodium silicate (48%): 104
	AAC-3 GGBFS + fly ash	*GGBFS: 71; fly ash: 283*	NaOH (50%): 21; sodium silicate (48%): 83
Mortar	CEM I	Clinker: 513	—
	CEM III/C	Clinker: 51.3; GGBFS: 461.7	—
	CEM VI (S-LL)	Clinker: 205.2; GGBFS: 205.2; limestone: 102.6	—
	AAS GGBFS	GGBFS: 470	Sodium silicate: 59; KOH (50%): 44

The concrete CEM I model uses a finished cement provider; CEM II/B-V and CEM III/B are represented by CEM I plus fly ash or GGBFS. The mortar models instead combine clinker with the stated supplementary constituents, without separate gypsum, cement grinding or blending exchanges. They are therefore simplified binder proxies, not inventories of finished cements. The CEM VI (S-LL) proxy contains 40% clinker, 40% GGBFS and 20% limestone by mass of the 513 kg binder input. CEM VI is specified in EN 197-5 [39]; the designation here does not certify compliance with all chemical, physical or constituent requirements. AAC-3 contains 71 kg GGBFS and 283 kg fly ash per m^3.

2.4. Life Cycle Inventory Database and Provider Mapping

The ten product systems were implemented and calculated in openLCA 2.6.2 [40]. BAFU-2025 Version 2—openLCA 9 March 2026 was used as the background life cycle inventory database [41]. The foreground processes carried a PL location label, whereas the linked background providers retained the CH or RER geographies recorded in the mapping. The results therefore represent the selected BAFU provider system and are not a fully regionalized Polish LCA.

CH providers were used for mixing plant infrastructure, diesel use in construction machinery, medium-voltage electricity, light fuel oil, natural gas, CEM I cement, tap water, sand, gravel, clinker, and limestone. RER providers were used for lubricating oil, freight, burdened GGBFS, sodium hydroxide, sodium silicate, and potassium hydroxide. Exact provider process names and locations are not reproduced in this manuscript.

Fly ash was linked to the custom process "FG/Material/Fly ash/zero burden-RER", whereas GGBFS was linked to "Ground granulated blast furnace slag, with burdens, at plant {RER}-RER". Thus, the GGBFS contribution is included in CEM III/B concrete and the slag-containing mortars and activated systems; CEM II/B-V contains fly ash rather than slag. The selected slag provider includes its assigned burdens, not necessarily the whole burden of ironmaking. Assigning all coke- and carbonate-related ironmaking emissions to slag would require a specified allocation rule and would risk double counting if added to an already burdened dataset. Conversely, zero upstream burden for fly ash is an assumption, not an

intrinsic material property. The allocation basis and composition of the slag provider require inspection before equivalent zero-burden, economic, mass allocation and provider-specific scenarios can be compared [25,26,42,43]. Such scenarios have not been run.

The model contains provider exchanges for NaOH, sodium silicate and KOH, but their equivalence to the recipe dosages is unverified. The NaOH provider represents a 50% aqueous product and sodium silicate liquor containing 48% solids. In the recipe, the 44 kg KOH exchange denotes a 50% solution, but the model links 44 kg mass-for-mass to a regional storage provider; its representation of solution concentration and production burden is unverified. Table 1 therefore reports entered exchanges, not corrected dry solid dosages. These mappings require correction in the model itself; changes to the text do not correct the reported LCIA totals.

A chemically equivalent correction must use m(solution) = m(dry solute)/w, where w is the solute mass fraction, and must reconcile the associated water. Thus 4 kg and 21 kg of NaOH pellets require 8 kg and 42 kg, respectively, of a 50% solution. The original mappings contain only 2 kg and 10.5 kg dry NaOH. A 44 kg, 50% KOH solution contains 22 kg KOH and 22 kg water; the correct provider exchange depends on whether the provider reference is dry KOH or solution. For the 48% solids silicate, water is 0.52 times the solution mass, but total solids alone do not determine the separate SiO_2 and Na_2O contents. These arithmetic identities are not revised LCA results.

Activator dosage as Na_2O requires the Na_2O contribution of each sodium-bearing input. Pure NaOH contributes approximately 0.7748 kg Na_2O equivalent per kg NaOH; hence dosage is $100 \times [0.7748\text{m(NaOH)} + \text{m}(Na_2O \text{ in silicate})]/\text{m(precursor)}$. The molar silicate modulus is $[\text{m}(SiO_2)/60.08]/[\text{m}(Na_2O)/61.98]$. KOH should be reported on a K_2O basis, separately from Na_2O, unless a clearly defined molar alkali equivalence convention is adopted. Table 2 reports an exchange-level mass balance of the original aqueous activator inputs: dry hydroxide and silicate solids, solution-carried water, and the nominal combined dry-solids-to-binder mass ratio. These calculations verify only the arithmetic implied by the stated concentrations. They do not establish supplier-specific oxide composition or total water-to-binder ratios, and they do not correct the openLCA inputs or impact totals. The sodium silicate solution's 48% total solids do not identify its separate Na_2O and SiO_2 fractions; product-specific composition and recalculation of the product systems are required before corrected dosages or LCIA results can be reported.

Table 2. Mass balance of the original aqueous activator exchanges.

System	Dry Hydroxide (kg/m^3)	Silicate Solids (kg/m^3)	Solution Water (kg/m^3)	Dry Activator/Binder (%)
AAC-1 GGBFS	2.00 (NaOH)	34.56	39.44	10.3
AAC-2 fly ash	52.00 (NaOH)	49.92	106.08	24.6
AAC-3 GGBFS + fly ash	10.50 (NaOH)	39.84	53.66	14.2
AAS GGBFS	22.00 (KOH)	28.32	52.68	10.7

Calculated from Table 1 using 50 wt% NaOH/KOH and 48 wt% total solids in sodium silicate. Solution water = 0.50 × hydroxide-solution mass + 0.52 × silicate-solution mass; dry activator/binder = (0.50 × hydroxide-solution mass + 0.48 × silicate-solution mass)/listed binder mass × 100. Solution water excludes separately added mixing water. The calculations describe the original exchanges; they are not corrected LCIA inputs. Total silicate solids cannot be divided into Na_2O and SiO_2 without product-specific composition.

2.5. Life Cycle Impact Assessment

Life cycle impact assessment used CML-IA baseline as implemented in openLCA LCIA methods 2.7.5 [44–46]. CML denotes the Institute of Environmental Sciences at Leiden University and IA denotes impact assessment. Each indicator is calculated by multiplying the solved elementary flow inventory by the corresponding characterization factors and summing within that category. The eleven indicators were:

- Abiotic depletion of elements (ADP-e), kg Sb eq;
- Abiotic depletion of fossil fuels (ADP-f), MJ;
- Acidification potential (AP), kg SO_2 eq;
- Eutrophication potential (EP), kg PO_4^{3-} eq;
- *Freshwater aquatic ecotoxicity potential (FAETP), kg 1,4-dichlorobenzene equivalents (kg 1,4-DB eq);*
- Global warming potential over 100 years (GWP100a), kg CO_2 eq;
- Human toxicity potential (HTP), kg 1,4-DB eq;
- Marine aquatic ecotoxicity potential (MAETP), kg 1,4-DB eq;
- Ozone layer depletion potential (ODP), kg CFC-11 eq;
- Photochemical oxidation potential (POCP), kg C_2H_4 eq; and
- Terrestrial ecotoxicity potential (TETP), kg 1,4-DB eq.

The toxicity and ecotoxicity unit, kg 1,4-DB eq, expresses a modeled potential relative to 1,4-dichlorobenzene; it is not a measured mass of that substance in the concrete or an estimate of site-specific harm. Similarly, kg Sb eq expresses abiotic resource depletion relative to antimony. Indicators with different reference substances and mechanisms must not be added or compared as absolute magnitudes. The factors and their units are defined by the selected CML implementation [44–46].

For reproducibility, let $q_{s,e}$ denote the solved amount of elementary flow e per m^3, and $CF_{c,e}$ its category-specific factor. Characterization gives $I_{s,c} = \Sigma_e q_{s,e} CF_{c,e}$. For ADP-e, extraction flows are multiplied by factors in kg Sb eq per kg extracted resource [45,46]. Process contributions then partition this characterized total as in Equation (1); CML is the characterization method and ADP-e one of its indicators. As an arithmetic example using the rounded manuscript results, concrete CEM I gives a clinker contribution of approximately $278.2 \times 0.886 = 246.5$ kg CO_2 eq per m^3. Its CEM II/B-V reduction is $100 \times (1 - 198.6/278.2) \approx 28.6\%$. These checks illustrate contribution and comparative metrics, not an independent reconstruction of the elementary flow inventory. A numerical ADP-e reconstruction requires the original extraction flows and matched factors, which cannot be recovered from the category ratios alone.

2.6. Process Contributions and Numerical Reconciliation

Each product system was exported from openLCA to a separate Excel workbook containing the calculation setup, inventory, total impacts and direct contributions. The "Impacts" sheet supplied category totals and the "Direct impact contributions" sheet supplied the signed process contributions used here.

The original analysis compared 110 category totals with the consolidated results and reported agreement at stored numerical precision. Process contributions were identified by process UUID, name and location; the reported matrices contained 4236–4242 process columns per system. A direct contribution is the characterized elementary flow result of a process scaled to its activity in the solved product system [40,47]. Summing these process contributions counts each scaled direct inventory once. By contrast, summing cumulative upstream totals for all nodes would count shared supply chains repeatedly and must not be used for reconciliation.

For system s, impact category c, and process p, the exported direct contribution is denoted x(s,c,p). Its sum was required to reproduce the corresponding total impact I(s,c):

$$I_{s,c} = \sum_{p=1}^{P_s} x_{s,c,p}. \quad (1)$$

where $I_{s,c}$ is the total cradle-to-gate LCIA result for product system s in impact category c (expressed in the category-specific unit per 1 m^3); $x_{s,c,p}$ is the direct characterized contribution of process p to that result, in the same unit; P_s is the number of process contributions in the solved product system; and s, c, and p denote the product system, impact category, and process indices, respectively.

The original numerical audit reported a maximum relative residual of 5.751×10^{-16} across 110 process sum checks. This establishes arithmetic agreement as reported for those exports, not independent validation of provider mappings, allocation or recipe equivalence. A reproducible reconciliation table must retain, for each system and category, the exported total, positive sum, negative sum, signed sum and residual at full precision.

2.7. Comparative Metrics and Burden-Shifting Classification

For each non-reference variant i in material group g, the GWP reduction relative to the CEM I system of the same group was calculated as:

$$R_{\mathrm{GWP},i,g} = 100\left(1 - \frac{\mathrm{GWP}_{i,g}}{\mathrm{GWP}_{\mathrm{CEM\,I},g}}\right). \quad (2)$$

where $R_{GWP,i,g}$ is the GWP reduction of variant i in material group g (%); $\mathrm{GWP_{i,g}}$ is the unrounded cradle-to-gate GWP of variant i (kg CO_2 eq m^{-3}); $\mathrm{GWP_{CEM\,I,g}}$ is the unrounded GWP of the CEM I reference in the same group and unit; i denotes a non-reference variant; and g denotes either concrete or mortar.

A positive value indicates a lower GWP than the group-specific reference. Relative indices for category c were calculated as:

$$RI_{i,c,g} = 100\frac{I_{i,c,g}}{I_{\mathrm{CEM\,I},c,g}}. \quad (3)$$

where $RI_{i,c,g}$ is the relative index of variant i in category c and material group g (%); $I_{i,c,g}$ is the unrounded LCIA result of that variant in the category-specific unit per 1 m^3; $I_{CEM\,I,c,g}$ is the corresponding unrounded result of the CEM I reference; and i, c, and g denote the variant, impact category, and material group indices, respectively. The ratio is dimensionless.

An index below 100% was classified as below the reference and an index above 100% as above it. The classification was based on unrounded values. The number of lower and higher categories was used only as a transparent burden-shifting descriptor; it was not treated as a score, because categories were neither normalized nor weighted.

Within each product group, variant a was defined as Pareto-dominating variant b when:

$$I_{a,c} \le I_{b,c} \quad \text{for all } c, \qquad I_{a,c} < I_{b,c} \quad \text{for at least one } c. \quad (4)$$

where $I_{a,c}$ and $I_{b,c}$ are the unrounded LCIA results of variants a and b in category c, expressed in the same category-specific unit; a and b are alternatives within the same material group; and c spans all eleven CML-IA baseline indicators. The first condition requires variant a to be no higher than variant b in every category, and the second requires it to be strictly lower in at least one category.

Pareto screening used the unrounded values of all eleven indicators, separately for concrete and mortar. A relation is reported only for the original fixed inventory. A non-dominated model is one for which no other model satisfies Equation (4); it is not thereby

a preferred construction material. Without scenario and uncertainty analysis, a small difference can reverse a relation. The 0.19% TETP difference between CEM III/B and concrete CEM I is therefore a numerical distinction, not demonstrated environmental superiority or inferiority.

2.8. Process Contribution and Hotspot Concentration Metrics

For a given category, a positive process contribution is a signed characterized result greater than zero and increases the net indicator; a negative contribution is below zero and decreases it. "Positive" and "negative" describe arithmetic signs, not favorable or unfavorable environmental outcomes. Negative values can represent credits or database corrections and must be interpreted from the underlying dataset. The signed sums are defined as:

$$P^{+}_{s,c} = \sum_{p} \max\left(x_{s,c,p}, 0\right), \qquad P^{-}_{s,c} = \sum_{p} \min\left(x_{s,c,p}, 0\right). \tag{5}$$

where $P^{+}{}_{s,c}$ is the sum of all positive process contributions for system s and category c; $P^{-}{}_{s,c}$ is the sum of all negative process contributions and is therefore non-positive; $\max(x_{s,c,p}, 0)$ retains only the positive part of a contribution; $\min(x_{s,c,p}, 0)$ retains only the negative part; and the index p covers all processes in the solved product system. Both sums use the same category-specific unit as $I_{s,c}$.

The net result is $I = P^{+} + P^{-}$, with $P^{-} \leq 0$. Negative entries are retained in the balance and excluded only from the positive contribution ranking. A positive process share divided by the net total can exceed its share of P^{+} when negative corrections reduce the denominator. The presence or absence of negative GWP entries must be checked from the category matrix; the reported net GWP must not be assumed to equal P^{+} merely because the table reports positive hotspots.

Three concentration metrics use the positive sum P^{+} as their denominator. D_1 measures the largest positive contribution and C_5 the cumulative contribution of the five largest positive entries. These metrics differ from the "Share of net GWP" column in Tables 3 and 4, which divides by the signed category total. D_1 and C_5 are calculated as:

$$D_{1,s,c} = \frac{\max_{p}\left(x_{s,c,p}, 0\right)}{P^{+}_{s,c}}, \qquad C_{5,s,c} = \frac{\sum_{k=1}^{5} x^{+}_{(k),s,c}}{P^{+}_{s,c}}, \tag{6}$$

where $D_{1,s,c}$ is the share of the largest positive process contribution in $P^{+}{}_{s,c}$; $C_{5,s,c}$ is the cumulative share of the five largest positive contributions; $x^{+}{}_{k;s,c}$ is the k-th largest positive process contribution after descending sorting; and k is the rank from 1 to 5. Both metrics are dimensionless fractions and were multiplied by 100 when reported as percentages.

Hotspot breadth N_{80} was calculated as the minimum number of positive process contributions required to reach 80% of P^{+}:

$$N_{80,s,c} = \min\left\{ n : \frac{\sum_{k=1}^{n} x^{+}_{(k),s,c}}{P^{+}_{s,c}} \geq 0.80 \right\}, \tag{7}$$

where $N_{80,s,c}$ is the smallest integer number of positive process contributions needed to reach at least 80% of $P^{+}{}_{s,c}$; n is the number of ranked contributions included in the cumulative sum; k is the rank index; $x^{+}{}_{k;s,c}$ is the k-th largest positive contribution; and 0.80 is the adopted cumulative share threshold. $N_{80,s,c}$ is therefore an integer count, not a percentage.

The 80% threshold is a descriptive cumulative share convention, not a statistical confidence level or a physical threshold. For each system, positive entries are sorted in descending order, accumulated and counted until their sum first reaches $0.80P^{+}$. The range 41–45 is the minimum-to-maximum count across the four activated models: AAC-1, 44; AAC-2, 41; AAC-3, 45; and AAS, 41. These entries may belong to shared supply chains. They must not

be interpreted as 41–45 independent opportunities for intervention. The metrics describe concentration, not sensitivity or uncertainty.

Table 3. GWP reductions and category directions relative to the product group reference.

Group	Variant	GWP Reduction (%)	Categories Below CEM I	Categories Above CEM I	Largest Relative Result (% of CEM I)
Concrete	CEM I	0.0	—	—	100
	CEM II/B-V	28.6	11	0	88 (ADP-e)
	CEM III/B	54.8	9	2	115 (ADP-e)
	AAC-1 GGBFS	67.8	4	7	534 (ADP-e)
	AAC-2 fly ash	52.2	3	8	1147 (ADP-e)
	AAC-3 GGBFS + fly ash	71.9	4	7	634 (ADP-e)
Mortar	CEM I	0.0	—	—	100
	CEM III/C	76.6	10	1	143 (ADP-e)
	CEM VI (S-LL)	53.1	10	1	114 (ADP-e)
	AAS GGBFS	64.2	4	7	802 (ADP-e)

Table 4. GWP hotspot concentration results.

Group	Variant	Leading Direct Process	Share of Net GWP (%)	C_5 (% of P^+)	N_{80}
Concrete	CEM I	Clinker, at plant (CH)	88.6	92.0	1
	CEM II/B-V	Clinker, at plant (CH)	86.7	90.7	1
	CEM III/B	Clinker, at plant (CH)	63.5	74.4	10
	AAC-1 GGBFS	Natural gas, industrial furnace (CH)	7.9	28.6	44
	AAC-2 fly ash	Natural gas, industrial furnace (CH)	7.8	26.9	41
	AAC-3 GGBFS + fly ash	Natural gas, industrial furnace (CH)	10.2	26.6	45
Mortar	CEM I	Clinker, at plant (CH)	91.2	93.9	1
	CEM III/C	Clinker, at plant (CH)	39.6	60.1	22
	CEM VI (S-LL)	Clinker, at plant (CH)	77.9	83.9	3
	AAS GGBFS	Natural gas, industrial furnace (CH)	12.4	30.6	41

3. Results

3.1. Global Warming Potential

The concrete GWP results ranged from 78.2 to 278.2 kg CO_2 eq m^{-3} (Figure 1a). Concrete CEM I had the highest value. CEM II/B-V reached 198.6 kg CO_2 eq m^{-3}, corresponding to a 28.6% reduction. CEM III/B reached 125.7 kg CO_2 eq m^{-3}, a reduction of 54.8%. The activated systems were 89.7 kg CO_2 eq m^{-3} for AAC-1 GGBFS, 132.9 kg CO_2 eq m^{-3} for AAC-2 fly ash, and 78.2 kg CO_2 eq m^{-3} for AAC-3 GGBFS + fly ash. Their reductions were 67.8%, 52.2%, and 71.9%, respectively. The GWP order was AAC-3 < AAC-1 < CEM III/B < AAC-2 < CEM II/B-V < CEM I.

Mortar GWP ranged from 101.2 to 433.1 kg CO_2 eq m^{-3} (Figure 1b). Relative to mortar CEM I, CEM III/C reduced GWP by 76.6%, CEM VI (S-LL) by 53.1%, and AAS GGBFS by 64.2%. The corresponding order was CEM III/C < AAS GGBFS < CEM VI (S-LL) < CEM I.

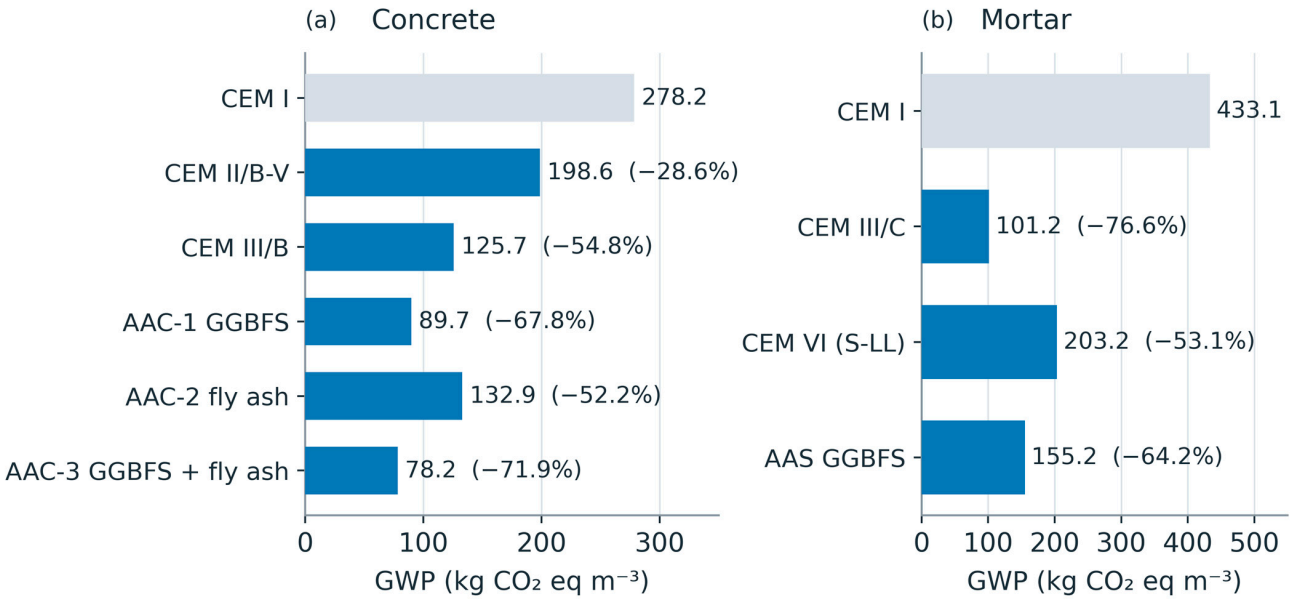


Figure 1. Cradle-to-gate global warming potential (GWP) for (a) concrete and (b) mortar models. Values in parentheses are reductions relative to CEM I within the same product group. The two groups use separate reference systems and are not treated as functionally equivalent.

3.2. Category Directions and Environmental Burden Shifting

GWP reduction did not imply a lower result in every category (Table 3 and Figure 2). CEM II/B-V was below concrete CEM I in all eleven categories. CEM III/B was below the reference in nine categories and above it in ADP-e and TETP. The unrounded TETP result was only 0.19% above the reference, whereas ADP-e was 15% higher.

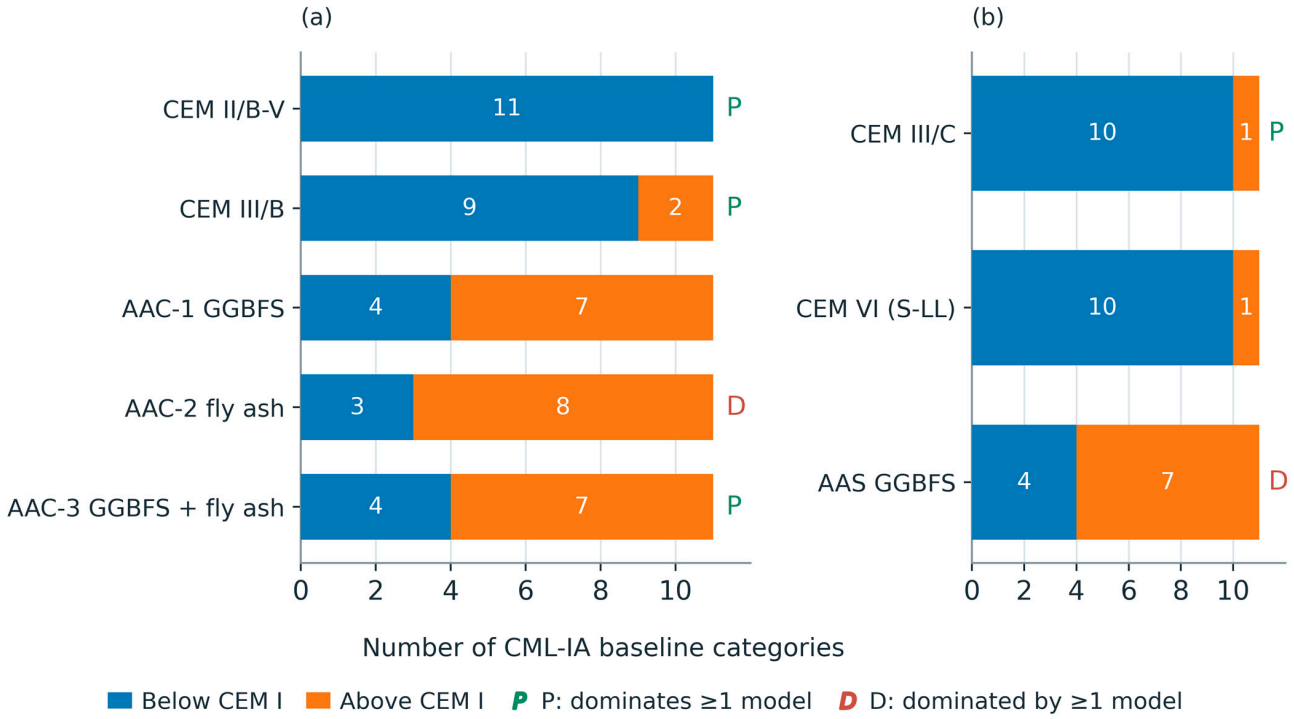


Figure 2. Number of CML-IA baseline categories below and above the CEM I result within each product group: (**a**) concrete and (**b**) mortar. P marks a model that Pareto-dominates at least one other model; D marks a model dominated by at least one other model under the original fixed inventory. Unmarked models show neither relation in the compared set. Counts are descriptive and are not a weighted environmental score.

The activated concretes produced more pronounced trade-offs. AAC-1 and AAC-3 were below CEM I in four categories and above it in seven. AAC-2 was below the reference in three categories and above it in eight. ADP-e generated the largest relative increase for all three activated concretes: 534% of CEM I for AAC-1, 1147% for AAC-2, and 634% for AAC-3. Their HTP indices were 212%, 402%, and 225%, respectively, and their TETP indices were 287%, 778%, and 355%.

Both low-clinker mortars were below mortar CEM I in ten categories. ADP-e was the only increase, reaching 143% of the reference for CEM III/C and 114% for CEM VI (S-LL). AAS GGBFS was below the reference in four categories—GWP, AP, EP, and POCP—and above it in seven. Its highest index was ADP-e at 802%; HTP and TETP reached 252% and 250%, respectively.

3.3. Pareto Dominance

The original fixed inventory yielded four conditional Pareto relations: CEM II/B-V below concrete CEM I in all indicators; CEM III/B below AAC-2 in all indicators; AAC-3 below AAC-2 in all indicators; and CEM III/C below AAS GGBFS in all indicators. These are model output relations under Equation (4), not robust rankings of physical materials. They have not been re-evaluated after correcting activator concentrations or varying allocation, transport and energy supply.

No dominance relation existed between CEM III/B and AAC-3. AAC-3 had lower GWP, AP, and POCP, whereas CEM III/B had lower results in several resource-, toxicity-, and ecotoxicity-related categories. Likewise, CEM III/C did not dominate CEM VI (S-LL), because the former had lower GWP and several other impacts but higher ADP-e. These non-dominated relationships are examples of genuine trade-offs within the indicator set; resolving them would require an explicit decision context rather than an implicit count or weighting.

3.4. GWP Process Hotspots and Contribution Concentration

The same reduction in total GWP could be associated with very different contribution structures (Table 4 and Figure 3). The two CEM I references were strongly concentrated: “Clinker, at plant” contributed 88.6% of net concrete CEM I GWP and 91.2% of net mortar CEM I GWP. One positive process was sufficient to exceed 80% of the positive GWP sum in both systems. CEM II/B-V remained similarly concentrated, with clinker contributing 86.7% of net GWP.

Replacing a larger clinker fraction broadened the profile. In CEM III/B, clinker remained the leading process at 63.5% of net GWP, but ten positive processes were required to reach 80% of P^+. In CEM III/C mortar, clinker contributed 39.6% and N_{80} increased to 22. CEM VI (S-LL), which retained 205.2 kg of clinker, was more concentrated: clinker contributed 77.9% and only three processes were required to reach 80%.

The activated systems were diffuse. Their leading GWP process was “Natural gas, burned in industrial furnace 1MWth {CH}”, with a net share of 7.9% in AAC-1, 7.8% in AAC-2, 10.2% in AAC-3, and 12.4% in AAS GGBFS. The five largest positive contributions together represented only 26.6–30.6% of P^+. Between 41 and 45 positive processes were required to reach 80% of P^+. The lower GWP of these systems therefore did not correspond to a single avoided or substitute process that controlled the remaining result; the residual burden was distributed across energy and chemical background chains.

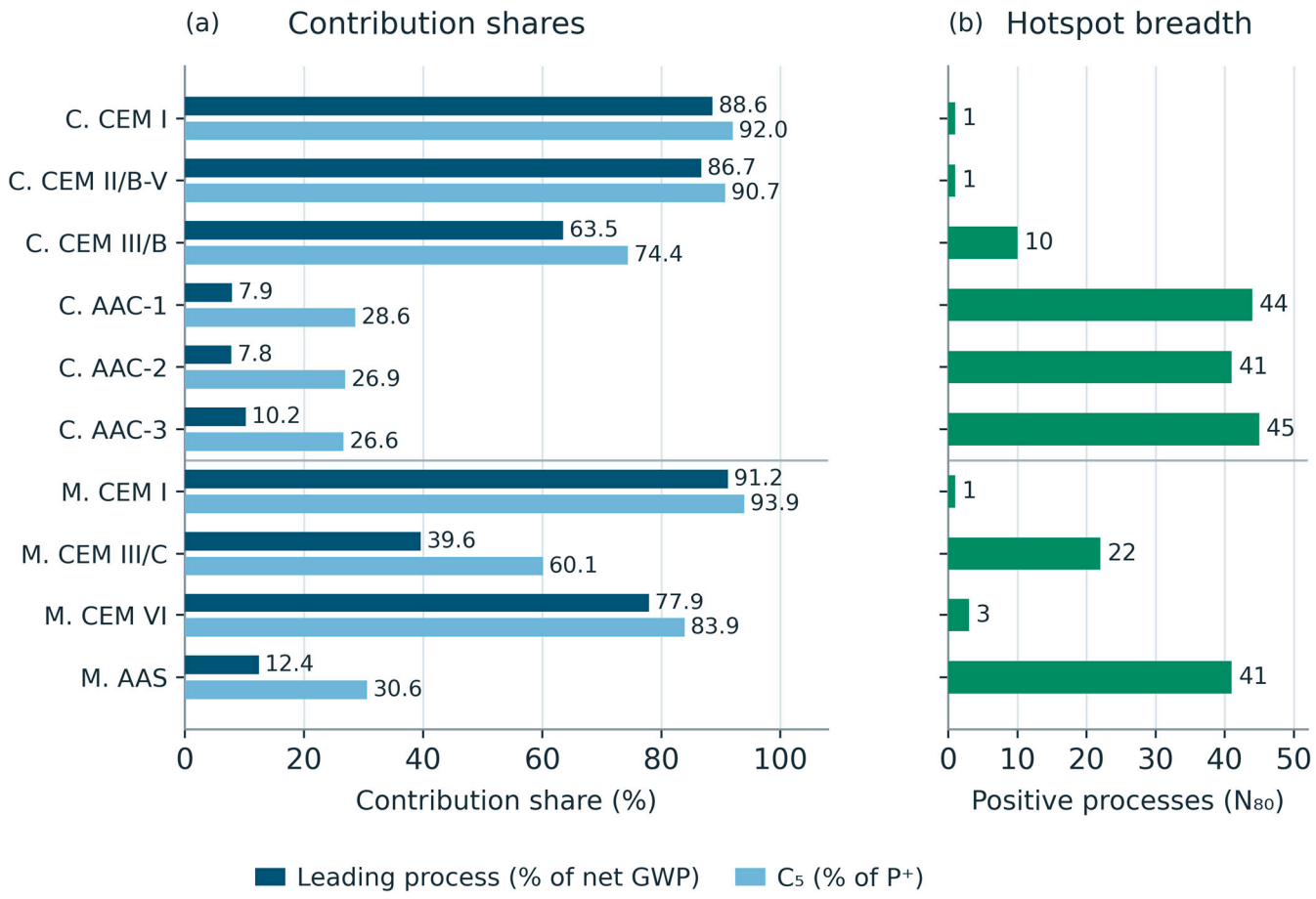


Figure 3. GWP process contribution metrics for the ten models: (**a**) separate bars show the leading positive process contribution as a share of net GWP and C_5, the combined share of the five largest positive contributions in P^+; the bars have different denominators and are not additive; (**b**) N_{80}, the number of positive process contributions required to reach 80% of P^+. C. denotes concrete and M. denotes mortar.

3.5. Resource, Toxicity, and Ecotoxicity Hotspots

The ADP-e contribution matrices contained both positive resource extraction contributions and a negative "Resource correction, PbZn, cadmium" process. The negative offset ranged from 21.3% to 38.4% of the positive contribution sum across the ten systems. "Zinc concentrate, at beneficiation" was the largest positive process, but its share of the net result reached 60.9–66.5% in the cement-based concretes because the negative correction reduced the denominator. When normalized to P^+, its share was 38.9–41.0%. This difference demonstrates why ADP-e hotspots should not be interpreted solely as percentages of a net total.

HTP was less concentrated than the clinker-controlled GWP of conventional systems. "Ferrochromium, high-carbon, 68% Cr, at plant" was the leading direct process in nine systems, contributing 18.5–28.9% of net HTP. Mortar CEM I was the exception: disposal of spoil from lignite mining contributed 17.4%, marginally above the 17.1% contribution of ferrochromium. For FAETP, lignite mining spoil disposal was the largest process in all ten systems, contributing 23.4–39.3% of the net result. MAETP was controlled mainly by spoil and tailings disposal processes, with the largest individual share ranging from 21.0% to 34.3%.

The mercury cell, sodium hydroxide and mercury supply processes together accounted for 46.6%, 72.4%, 60.7% and 32.3% of the original TETP results for AAC-1, AAC-2, AAC-3 and AAS GGBFS, respectively (Figure 4). Their presence concerns the modeled background

chemical supply chain; it does not indicate that mercury was added to the concrete or mortar. The NaOH production mix provider links to a mercury cell process in the solved network. For AAS GGBFS, which has KOH and sodium silicate as foreground activators, the specific path to the NaOH process has not been established. The aggregate contribution matrix cannot identify that path; a provider link trace is required. No membrane cell or supplier-specific replacement has been calculated.

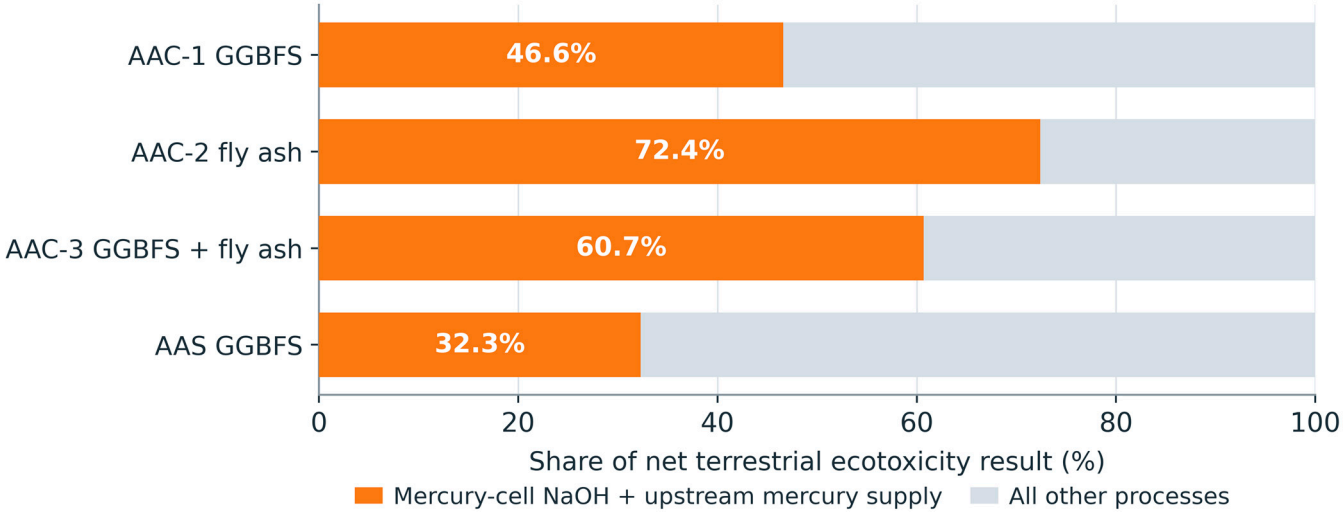


Figure 4. Combined shares of the sodium hydroxide mercury cell process and its upstream mercury supply process in the net terrestrial ecotoxicity potential (TETP) of four activated systems. The remaining share represents all other processes in the solved process contribution matrix. The mercury-related shares are specific to the selected provider model.

3.6. Exchange-Level Activator Mass Balance

Using the concentrations reported for the original providers, the exchanges correspond to 2.00–52.00 kg m^{-3} of dry hydroxide, 28.32–49.92 kg m^{-3} of sodium silicate solids, and 39.44–106.08 kg m^{-3} of solution-carried water (Table 2). The nominal combined dry activator-to-binder ratio ranges from 10.3% to 24.6%. For AAC-1 and AAC-3, the original NaOH solution exchanges contain 2.00 and 10.50 kg m^{-3} of dry NaOH, respectively, compared with 4 and 21 kg m^{-3} of NaOH pellets in the cited recipes. Thus, the original provider exchanges represent half the recipe dry-NaOH mass for these two systems. This check identifies an exchange mass mismatch; it does not establish sodium silicate oxide composition or recalculate the LCIA results.

4. Discussion

4.1. Carbon Reduction and the Structure of GWP

All alternatives had lower GWP than their own CEM I reference in the original model. This pattern is consistent with the established role of clinker substitution [2–5,10–13], but the magnitudes cannot yet be attributed solely to binder chemistry. In particular, the concrete reference uses a cement provider whereas the mortar reference uses clinker, and the activated inventories contain concentration mismatches. The process results nevertheless identify clinker as the principal original GWP contributor in both references and in CEM II/B-V. This is a basis for checking the inventory rather than proof that the reported reduction percentages transfer to actual products.

The relationship becomes less concentrated as clinker is replaced. CEM III/B and CEM III/C retained clinker as the leading GWP process, but the shares fell to 63.5% and 39.6%. GGBFS-related, energy, transport, and other background processes formed a larger fraction

of the remaining total. This broadening is not an environmental disadvantage by itself, it indicates that further GWP improvement cannot be estimated from clinker content alone. It also helps explain why low-clinker materials with similar total GWP can respond differently to changes in energy.

Within the concrete group, AAC-3 had the lowest modeled GWP at 78.2 kg CO_2 eq m^{-3}, 71.9% below concrete CEM I (278.2 kg CO_2 eq m^{-3}). Within the mortar group, CEM III/C had the lowest modeled GWP at 101.2 kg CO_2 eq m^{-3}, 76.6% below mortar CEM I (433.1 kg CO_2 eq m^{-3}). These are separate 1 m^3 cradle-to-gate outputs under the original provider mappings and activator exchanges, the common freight exchange, and no additional curing energy input; performance equivalence was not verified. The activated models also had diffuse contribution profiles: the leading positive process contributed 7.8–12.4% of net GWP, and more than forty positive processes were required to reach 80% of P^+. This makes the modeled GWP results explicit while limiting their interpretation to the stated inventory.

4.2. Burden Shifting and Pareto Screening

The direction counts separate relatively consistent improvement from pronounced burden shifting. CEM II/B-V was lower than CEM I in every indicator. CEM III/B, CEM III/C, and CEM VI (S-LL) were lower in nine or ten categories, with ADP-e as the recurring exception. In contrast, the four activated systems were lower in only three or four categories and higher in seven or eight. This pattern is consistent with previous observations that alkali-activated materials can combine low GWP with higher resource, toxicity, ecotoxicity, or ozone depletion indicators [12,13,28–34,48,49].

Category counts are descriptive, not a sustainability score. Changes in indicators with different mechanisms cannot be offset against one another without an explicit weighting method. Pareto screening retains all eleven inequalities, whereas a count retains only the direction of change relative to CEM I. The reported relations for AAC-2 and AAS GGBFS therefore describe the full original indicator set but remain dependent on inventory validity and do not carry greater evidential certainty than the underlying inputs.

Dominance remains conditional on the fixed model. A change in by-product allocation, provider geography, transport, activator technology, or declared unit could remove or create a dominance relation. The present findings show which alternatives are dominated under the documented assumptions; they do not establish universal technological rankings. Non-dominated variants also require careful interpretation. AAC-1 and AAC-3 remained non-dominated because their low GWP, AP, or POCP results coexisted with higher resource- and toxicity-related results. A decision among them and low-clinker cement systems would require explicit priorities, technical performance evidence, and a defined application.

4.3. Interpretation of Toxicity and Resource Hotspots

The process matrices provide evidence for several non-GWP hotspots that could only be hypothesized from total results. The large TETP shares of the sodium hydroxide, mercury cell and mercury supply processes show that the activated system TETP results depend strongly on the chemical production technology represented in the selected background database. This is not a general claim that all sodium hydroxide currently used for activation is produced by mercury cell technology. It is a model-specific finding and a clear target for provider verification or future scenario analysis.

AAC-2 had both the largest activator quantities and the highest TETP of the concrete group. The two named mercury-related processes contributed 72.4% of its net TETP. AAC-3 used smaller activator quantities and had a lower total TETP, although the combined share remained 60.7%. These results support the broader literature conclusion that acti-

vator formulation and inventory selection materially influence alkali-activated material LCAs [12,13,29,30,32–36,48,49]. They also demonstrate why simply assigning zero upstream burden to fly ash does not make a fly ash-rich activated system uniformly favorable.

ADP-e includes positive resource contributions and a negative database correction; percentages of the net total must therefore be distinguished from percentages of P^+. The "Resource correction, PbZn, cadmium" entry is not evidence of physical resource generation or a measured benefit of the binder. It is part of the database accounting represented in this calculation. Toxicity and resource depletion indicators also depend on characterization models and elementary flow mapping [45,46]. They are screening indicators, not site-specific risk assessments. Comparison with another LCIA method would require recalculating the same inventories with that method and cannot be inferred by rescaling the CML totals.

The toxicity and aquatic ecotoxicity matrices also show that the leading processes can be remote from the foreground mixture names. Ferrochromium production and disposal of mining spoil or tailings dominated several indicators. These processes occur in background chains connected to energy, chemicals, infrastructure, and material production. The contribution analysis identifies them as direct characterized processes in the solved product system; it does not by itself establish which first-tier exchange should receive the entire burden. A supply chain path or scenario analysis would be required for that attribution.

4.4. Comparison with Published Mixture-Level LCAs

Garces et al. [14] provide the recipe provenance for three concrete models, but the present NaOH solution mapping does not preserve the dry NaOH dosage of the source. Differences between the studies also concern geography, databases and precursor allocation. Accordingly, the source is used to document provenance, not to validate the current reduction percentages. Numerical agreement or disagreement between models with different chemical dosages cannot isolate the environmental effect of a database or allocation choice.

Tait and Cheung [15] provide a partially comparable cradle-to-gate design for CEM I, CEM II/B-V, and CEM III/B concrete. Their UK inventory and assessment methods differ from the present BAFU/CML implementation. Jiang et al. [16] compared conventional and activated concrete and mortar, but their recipes and inventory representation are also different. These studies support the use of defined mixture-level comparisons but reinforce the need to report providers, allocation assumptions, and contribution structure before transferring numerical results.

The literature identifies inventory completeness and geography [17–20,23,24], allocation of fly ash and GGBFS [21,22,25–27,42,43], and activator production and transport [28–36,48–51] as consequential choices. The current case study makes several of these choices visible, but it does not demonstrate their equivalence across recipes or their insignificance for the outcome. Its numerical outputs remain specific to the original provider network.

The systematic review by Nikravan et al. [12] found broad variation in both reported benefits and methods for alkali-activated material LCA. The process concentration metrics used here provide an additional way to describe that methodological exposure. A clinker-dominated GWP result can be expected to respond strongly to the clinker dataset and clinker mass, whereas a diffuse activated system profile can respond to several linked chemical and energy providers. The metrics do not measure uncertainty, but they identify where uncertainty and sensitivity work would be most informative.

4.5. Practical Implications

The practical use of the present analysis is to prioritize inventory verification. For clinker-rich systems, verify cement composition and the distinction between clinker and

finished cement before quantifying substitution benefits. For slag- and fly ash-containing systems, establish consistent allocation and constituent processing. For activated systems, first reconcile dry alkali, silicate solids and solution water, then verify the activator technology and energy supply. Figure 5 illustrates why a GWP-only screen is insufficient: several original low-GWP models have substantially higher ADP-e. The plot supports identification of questions for model revision; it does not establish a preferred binder.

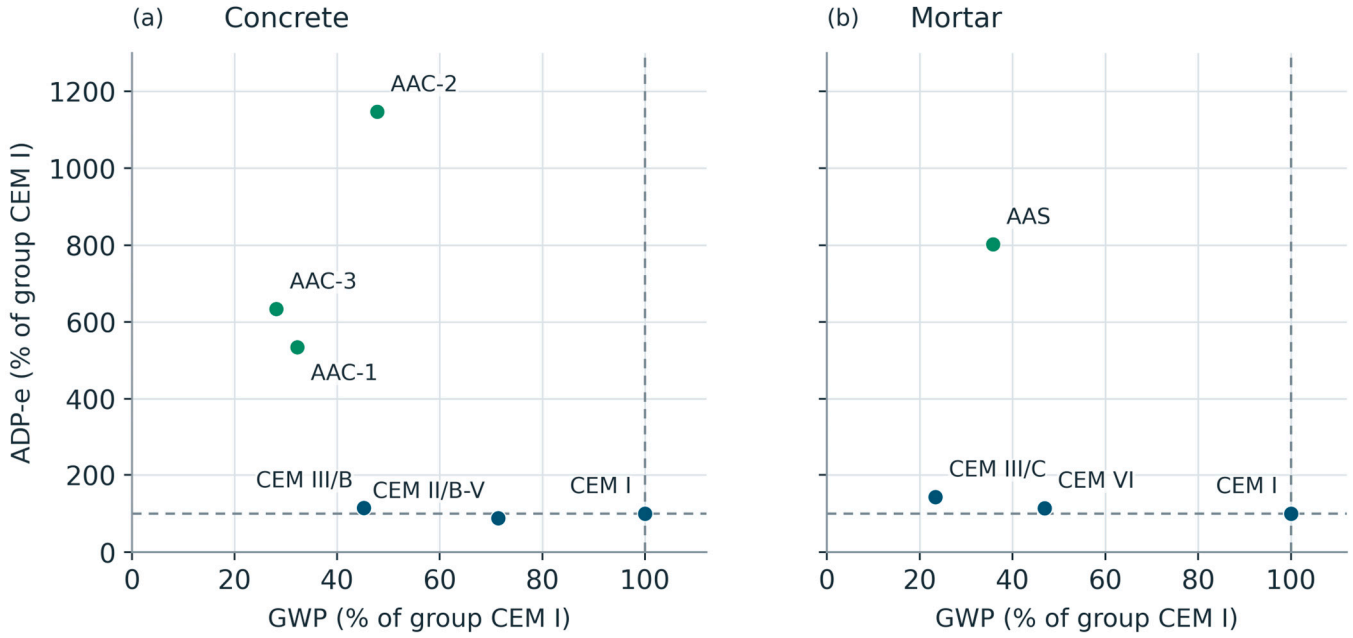


Figure 5. GWP and abiotic depletion of elements (ADP-e) relative to the group-specific CEM I reference: (**a**) concrete and (**b**) mortar. GWP percentages are derived from the reductions reported in Section 3.1; ADP-e values are the rounded indices reported in Section 3.2 and Table 3. Both axes use a linear scale, and dashed lines mark the reference value of 100%. This two-indicator comparison does not establish Pareto dominance or robustness to corrected inventory mappings.

For an engineering decision, the inventory should be recalculated for actual suppliers and transport routes, including verified curing energy. Within-group Pareto screening should then be repeated for each scenario. A relation that persists across the selected scenarios is more informative than a relation from one deterministic inventory, although it still requires performance equivalence. The current results cannot demonstrate such persistence.

Material selection additionally requires a specified performance: at least 28-day compressive strength, density, water-to-binder definition, workability and curing regime, followed by exposure-appropriate durability evidence. For activated binders, solution water and activator solids must be included consistently in the reported ratios. Neither these verified data for all ten formulations nor a service life comparison are provided here. The volumetric outputs therefore cannot justify structural substitution, equal service life or whole life environmental superiority [18,21,52].

4.6. Limitations

The analysis is limited to a cradle-to-gate boundary and one deterministic inventory model. Construction, use, maintenance, repair, end of life, carbonation, and recycling were excluded. The foreground label PL did not regionalize all background processes to Poland; CH and RER providers were retained. A common freight exchange was used instead of constituent-specific distances.

The zero-burden fly ash and burdened slag assumptions are asymmetric. No allocation, transport, electricity/heat, alternative activator technology or alternative LCIA method

scenario has been calculated. More fundamentally, the mass-for-mass NaOH and KOH mappings and the use of clinker instead of finished cement in mortar require inventory correction. These are unresolved model validity issues, not merely statistical uncertainty. They can change both impact magnitudes and Pareto relations. Numerical recalculation is necessary before presenting the reported differences as validated environmental comparisons.

The hotspot metrics are deterministic descriptors, not statistical measures. D_1, C_5, and N_{80} show concentration within the solved contribution matrix; they do not quantify data quality, uncertainty, or causal dependence among background processes. Process names identify direct characterized processes, but the analysis did not trace every hotspot to a unique first-tier foreground exchange.

The comparison also lacks verified technical equivalence and curing requirements for all ten mixtures. The 1 m^3 declared unit is a volumetric reference only. Provider-specific toxicity and resource results cannot be generalized to the binder classes, and arithmetic reconciliation does not remedy missing foreground information.

5. Conclusions

The case study links original cradle-to-gate category totals with signed process contributions for six concrete and four mortar inventory models. Its contribution is an interpretation procedure that distinguishes concentrated clinker-related GWP from dispersed chemical and energy supply chain contributions, while retaining cross-category trade-offs.

Under the original fixed inventory model, AAC-3 had the lowest GWP among concretes (78.2 kg CO_2 eq m^{-3}; 71.9% below concrete CEM I at 278.2 kg CO_2 eq m^{-3}), while CEM III/C had the lowest GWP among mortars (101.2 kg CO_2 eq m^{-3}; 76.6% below mortar CEM I at 433.1 kg CO_2 eq m^{-3}). These are separate per-1 m^3 cradle-to-gate comparisons using the original provider mappings and activator exchanges, the common freight exchange, and no additional curing energy. They do not establish equal strength, workability, durability, or service life. The unresolved activator mappings and binder representation make these provisional model outputs rather than validated product benefits. Activated models nevertheless exceeded their references in seven or eight indicators.

Four Pareto relations were identified for the original eleven-indicator dataset. Their robustness is untested, and they must be recalculated after correcting activator dosages and cement representation and assessing allocation, transport, energy and provider scenarios. They do not establish a universal material ranking.

The original clinker contributions were 88.6% and 91.2% of net GWP in concrete and mortar CEM I. In the activated models, the leading process contributed 7.8–12.4%, while 41–45 ranked positive entries were required to reach 80% of P^+. These linked background processes identify where inventory examination is needed; the count is not the number of independent mitigation measures. Mercury-related TETP hotspots likewise require chemical provider verification.

For engineering practice, AAC-3 is the lowest GWP concrete model and CEM III/C is the lowest GWP mortar model only under the stated original assumptions. The result cannot be transferred across concrete and mortar or to products with different strength, workability, durability, curing, suppliers, allocation rules, or transport routes. Before these outputs can guide material selection, the inventories must be made chemically consistent, technical performance must be verified, and supplier-specific scenarios must be recalculated across the relevant impact categories. Until those checks are completed, the reported values identify candidates for model correction; they do not substantiate a general selection of one binder system over another.

Author Contributions: Conceptualization, M.M., B.Ł.-P., P.M. and R.D.; methodology, M.M., B.Ł.-P. and R.D.; software, M.M. and R.D.; validation, M.M. and P.M.; formal analysis, M.M. and P.M.; investigation, M.M. and B.Ł.-P.; resources, M.M., B.Ł.-P. and P.M.; data curation, M.M. and R.D.; writing—original draft preparation, M.M. and B.Ł.-P.; writing—review and editing, B.Ł.-P. and P.M.; visualization, P.M. and B.Ł.-P.; supervision, B.Ł.-P.; project administration, B.Ł.-P. All authors have read and agreed to the published version of the manuscript.

Funding: This research received no external funding.

Institutional Review Board Statement: Not applicable.

Informed Consent Statement: Not applicable.

Data Availability Statement: The article reports selected aggregate LCIA results and the principal binder and activator exchanges in Table 1. No supplementary files accompany this submission. Full precision LCIA totals, complete per-mixture compositions and provider mappings, process contribution matrices, scripts, source file hashes, and validation records are not included. The corresponding author may be contacted to inquire about access to foreground openLCA models and additional documentation; any sharing is subject to their availability and the applicable BAFU database license. Background BAFU data are not redistributed.

Acknowledgments: The authors acknowledge the use of the openLCA software and the BAFU life cycle inventory database in preparing the environmental models.

Conflicts of Interest: The authors declare no conflicts of interest.

References

1. Andrew, R.M. Global CO_2 emissions from cement production. *Earth Syst. Sci. Data* **2018**, *10*, 195–217. [CrossRef]
2. Habert, G.; Miller, S.A.; John, V.M.; Provis, J.L.; Favier, A.; Horvath, A.; Scrivener, K.L. Environmental impacts and decarbonization strategies in the cement and concrete industries. *Nat. Rev. Earth Environ.* **2020**, *1*, 559–573. [CrossRef]
3. Scrivener, K.L.; John, V.M.; Gartner, E.M. Eco-efficient cements: Potential economically viable solutions for a low-CO_2 cement-based materials industry. *Cem. Concr. Res.* **2018**, *114*, 2–26. [CrossRef]
4. Miller, S.A.; John, V.M.; Pacca, S.A.; Horvath, A. Carbon dioxide reduction potential in the global cement industry by 2050. *Cem. Concr. Res.* **2018**, *114*, 115–124. [CrossRef]
5. Gartner, E.; Hirao, H. A review of alternative approaches to the reduction of CO_2 emissions associated with the manufacture of the binder phase in concrete. *Cem. Concr. Res.* **2015**, *78*, 126–142. [CrossRef]
6. Lothenbach, B.; Scrivener, K.; Hooton, R.D. Supplementary cementitious materials. *Cem. Concr. Res.* **2011**, *41*, 1244–1256. [CrossRef]
7. Juenger, M.C.G.; Snellings, R.; Bernal, S.A. Supplementary cementitious materials: New sources, characterization, and performance insights. *Cem. Concr. Res.* **2019**, *122*, 257–273. [CrossRef]
8. Shi, C.; Fernández-Jiménez, A.; Palomo, A. New cements for the 21st century: The pursuit of an alternative to Portland cement. *Cem. Concr. Res.* **2011**, *41*, 750–763. [CrossRef]
9. Provis, J.L. Alkali-activated materials. *Cem. Concr. Res.* **2018**, *114*, 40–48. [CrossRef]
10. Habert, G.; d'Espinose de Lacaillerie, J.B.; Roussel, N. An environmental evaluation of geopolymer-based concrete production: Reviewing current research trends. *J. Clean. Prod.* **2011**, *19*, 1229–1238. [CrossRef]
11. Turner, L.K.; Collins, F.G. Carbon dioxide equivalent emissions: A comparison between geopolymer and OPC cement concrete. *Constr. Build. Mater.* **2013**, *43*, 125–130. [CrossRef]
12. Nikravan, M.; Firdous, R.; Stephan, D. Life cycle assessment of alkali-activated materials: A systematic literature review. *Low-Carbon Mater. Green Constr.* **2023**, *1*, 13. [CrossRef]
13. Bajpai, R.; Choudhary, K.; Srivastava, A.; Sangwan, K.S.; Singh, M. Environmental impact assessment of fly ash and silica fume based geopolymer concrete. *J. Clean. Prod.* **2020**, *254*, 120147. [CrossRef]
14. Garces, J.I.T.; Tan, R.R.; Beltran, A.B.; Ongpeng, J.M.C.; Promentilla, M.A.B. Environmental life cycle assessment of alkali-activated material with different mix designs and self-healing agents. *Chem. Eng. Trans.* **2021**, *88*, 835–840. [CrossRef]
15. Tait, M.W.; Cheung, W.M. A comparative cradle-to-gate life cycle assessment of three concrete mix designs. *Int. J. Life Cycle Assess.* **2016**, *21*, 847–860. [CrossRef]
16. Jiang, M.; Chen, X.; Rajabipour, F.; Hendrickson, C.T. Comparative life cycle assessment of conventional, glass powder, and alkali-activated slag concrete and mortar. *J. Infrastruct. Syst.* **2014**, *20*, 04014020. [CrossRef]

17. Vieira, D.R.; Calmon, J.L.; Coelho, F.Z. Life cycle assessment applied to the manufacturing of common and ecological concrete: A review. *Constr. Build. Mater.* **2016**, *124*, 656–666. [CrossRef]
18. Van den Heede, P.; De Belie, N. Environmental impact and life cycle assessment of traditional and "green" concretes: Literature review and theoretical calculations. *Cem. Concr. Compos.* **2012**, *34*, 431–442. [CrossRef]
19. Gursel, A.P.; Masanet, E.; Horvath, A.; Stadel, A. Life-cycle inventory analysis of concrete production: A critical review. *Cem. Concr. Compos.* **2014**, *51*, 38–48. [CrossRef]
20. Flower, D.J.M.; Sanjayan, J.G. Green house gas emissions due to concrete manufacture. *Int. J. Life Cycle Assess.* **2007**, *12*, 282–288. [CrossRef]
21. Arrigoni, A.; Panesar, D.K.; Duhamel, M.; Opher, T.; Saxe, S.; Posen, I.D.; MacLean, H.L. Life cycle greenhouse gas emissions of concrete containing supplementary cementitious materials: Cut-off vs. substitution. *J. Clean. Prod.* **2020**, *263*, 121465. [CrossRef]
22. Hafez, H.; Kurda, R.; Cheung, W.M.; Nagaratnam, B. Comparative life cycle assessment between imported and recovered fly ash for blended cement concrete in the UK. *J. Clean. Prod.* **2020**, *244*, 118722. [CrossRef]
23. Colangelo, F.; Forcina, A.; Farina, I.; Petrillo, A. Life cycle assessment of different kinds of concrete containing waste for sustainable construction. *Buildings* **2018**, *8*, 70. [CrossRef]
24. Alkhawaldeh, A.A.; Judah, H.I.; Shammout, D.Z.; Almomani, O.A.; Alkhawaldeh, M.A. Sustainability evaluation and life cycle assessment of concretes including pozzolanic by-products and alkali-activated binders. *Results Eng.* **2024**, *23*, 102569. [CrossRef]
25. Saade, M.R.M.; da Silva, M.G.; Gomes, V. Appropriateness of environmental impact distribution methods to model blast furnace slag recycling in cement making. *Resour. Conserv. Recycl.* **2015**, *99*, 40–47. [CrossRef]
26. Habert, G. A method for allocation according to the economic behaviour in the EU-ETS for by-products used in cement industry. *Int. J. Life Cycle Assess.* **2013**, *18*, 113–126. [CrossRef]
27. Teh, S.H.; Wiedmann, T.; Castel, A.; de Burgh, J. Hybrid life cycle assessment of greenhouse gas emissions from cement, concrete and geopolymer concrete in Australia. *J. Clean. Prod.* **2017**, *152*, 312–320. [CrossRef]
28. Salas, D.A.; Ramirez, A.D.; Ulloa, N.; Baykara, H.; Boero, A.J. Life cycle assessment of geopolymer concrete. *Constr. Build. Mater.* **2018**, *190*, 170–177. [CrossRef]
29. Komkova, A.; Habert, G. Environmental impact assessment of alkali-activated materials: Examining impacts of variability in constituent production processes and transportation. *Constr. Build. Mater.* **2023**, *363*, 129032. [CrossRef]
30. Patrisia, Y.; Law, D.W.; Gunasekara, C.; Wardhono, A. Life cycle assessment of alkali-activated concretes under marine exposure in an Australian context. *Environ. Impact Assess. Rev.* **2022**, *96*, 106813. [CrossRef]
31. Munir, Q.; Abdulkareem, M.; Horttanainen, M.; Kärki, T. A comparative cradle-to-gate life cycle assessment of geopolymer concrete produced from industrial side streams in comparison with traditional concrete. *Sci. Total Environ.* **2023**, *865*, 161230. [CrossRef] [PubMed]
32. Abdulkareem, M.; Havukainen, J.; Nuortila-Jokinen, J.; Horttanainen, M. Environmental and economic perspective of waste-derived activators on alkali-activated mortars. *J. Clean. Prod.* **2021**, *280*, 124651. [CrossRef]
33. Mellado, A.; Catalán, C.; Bouzón, N.; Borrachero, M.V.; Monzó, J.M.; Payá, J. Carbon footprint of geopolymeric mortar: Study of the contribution of the alkaline activating solution and assessment of an alternative route. *RSC Adv.* **2014**, *4*, 23846–23852. [CrossRef]
34. Habert, G.; Ouellet-Plamondon, C. Recent update on the environmental impact of geopolymers. *RILEM Tech. Lett.* **2016**, *1*, 17–23. [CrossRef]
35. Fawer, M.; Concannon, M.; Rieber, W. Life cycle inventories for the production of sodium silicates. *Int. J. Life Cycle Assess.* **1999**, *4*, 207–212. [CrossRef]
36. Yang, K.-H.; Song, J.-K.; Song, K.-I. Assessment of CO_2 reduction of alkali-activated concrete. *J. Clean. Prod.* **2013**, *39*, 265–272. [CrossRef]
37. *ISO 14040:2006*; Environmental Management—Life Cycle Assessment—Principles and Framework. ISO: Geneva, Switzerland, 2006.
38. *ISO 14044:2006*; Environmental Management—Life Cycle Assessment—Requirements and Guidelines. ISO: Geneva, Switzerland, 2006.
39. *EN 197-5:2021*; European Committee for Standardization. Cement—Part 5: Portland-Composite Cement CEM II/C-M and Composite Cement CEM VI. CEN: Brussels, Belgium, 2021. Available online: https://knowledge.bsigroup.com/products/cement-portland-composite-cement-cem-ii-c-m-and-composite-cement-cem-vi (accessed on 12 October 2026).
40. GreenDelta. openLCA 2 Manual. Available online: https://greendelta.github.io/openLCA2-manual/ (accessed on 31 July 2026).
41. Swiss Federal Office for the Environment. BAFU Life Cycle Inventory Database. Available online: https://nexus.openlca.org/database/BAFU (accessed on 31 July 2026).
42. Seto, K.E.; Churchill, C.J.; Panesar, D.K. Influence of fly ash allocation approaches on the life cycle assessment of cement-based materials. *J. Clean. Prod.* **2017**, *157*, 65–75. [CrossRef]
43. Weidema, B.P. Avoiding co-product allocation in life-cycle assessment. *J. Ind. Ecol.* **2000**, *4*, 11–33. [CrossRef]

44. GreenDelta. openLCA LCIA Methods. Available online: https://nexus.openlca.org/database/openLCA%20LCIA%20Methods (accessed on 31 July 2026).
45. Leiden University, Institute of Environmental Sciences. CML-IA Characterisation Factors. Available online: https://www.universiteitleiden.nl/en/research/research-output/science/cml-ia-characterisation-factors (accessed on 31 July 2026).
46. Guinée, J.B.; Gorrée, M.; Heijungs, R.; Huppes, G.; Kleijn, R.; de Koning, A.; van Oers, L.; Wegener Sleeswijk, A.; Suh, S.; Udo de Haes, H.A.; et al. *Handbook on Life Cycle Assessment: Operational Guide to the ISO Standards*; Kluwer Academic Publishers: Dordrecht, The Netherlands, 2002. [CrossRef]
47. GreenDelta. Direct Contributions. Inter-Process Communication with openLCA. Available online: https://greendelta.github.io/openLCA-ApiDoc/results/impacts/direct-contributions.html (accessed on 12 October 2026).
48. Passuello, A.; Rodríguez, E.D.; Hirt, E.; Longhi, M.; Bernal, S.A.; Provis, J.L.; Kirchheim, A.P. Evaluation of the potential improvement in the environmental footprint of geopolymers using waste-derived activators. *J. Clean. Prod.* **2017**, *166*, 680–689. [CrossRef]
49. Faridmehr, I.; Nehdi, M.L.; Nikoo, M.; Huseien, G.F.; Ozbakkaloglu, T. Life-cycle assessment of alkali-activated materials incorporating industrial byproducts. *Materials* **2021**, *14*, 2401. [CrossRef] [PubMed]
50. Lolli, F.; Kurtis, K.E. Life cycle assessment of alkali-activated materials: Preliminary investigation for pavement applications. *RILEM Tech. Lett.* **2021**, *6*, 124–130. [CrossRef]
51. McLellan, B.C.; Williams, R.P.; Lay, J.; van Riessen, A.; Corder, G.D. Costs and carbon emissions for geopolymer pastes in comparison to ordinary Portland cement. *J. Clean. Prod.* **2011**, *19*, 1080–1090. [CrossRef]
52. Damineli, B.L.; Kemeid, F.M.; Aguiar, P.S.; John, V.M. Measuring the eco-efficiency of cement use. *Cem. Concr. Compos.* **2010**, *32*, 555–562. [CrossRef]

Disclaimer/Publisher's Note: The statements, opinions and data contained in all publications are solely those of the individual author(s) and contributor(s) and not of MDPI and/or the editor(s). MDPI and/or the editor(s) disclaim responsibility for any injury to people or property resulting from any ideas, methods, instructions or products referred to in the content.